H1prelim-09-171

ZEUS-prel-09-015

Combination of $F_2^{c\bar{c}}$ from DIS measurements at HERA

HERA Heavy Flavour Combination Group

Abstract

The charm contribution $F_2^{c\bar{c}}$ to the proton structure F_2 is determined by the HERA Heavy Flavour Group. The results of the D-meson production cross-section measurements are combined with the measurements using semi-leptonic decays into muons as well as the inclusive track measurements. The correlations of the systematic uncertainties between different measurements are taken into account. The data cover the kinematic range of photon virtuality $2 < Q^2 < 1000\,GeV^2$ and Bjorken scaling variable $10^{-5} < x < 10^{-1}$.

1 Introduction

Several results on the measurement of the charm contribution $F_2^{c\bar{c}}$ to the proton structure function F_2 at HERA have been published by the ZEUS [1, 3, 4, 5] and H1 [6, 7, 8, 9] collaborations. These data have shown clear evidence that the dynamics of charm production in ep scattering is dominated by the photon gluon fusion process. In this framework the process $e^+p \to e^+c\bar{c}X$ is sensitive to the gluon density in the proton [10] and allows its universality to be tested. The current analysis uses published and preliminary data from the HERA-I and HERA-II running periods. The averaged $F_2^{c\bar{c}}$ is obtained combining the D-meson measurements and the results of the displaced track and semi-leptonic decay analyses. The results are compared to different approaches of perturbative QCD (pQCD).

2 Data Samples

In the following the data sets used in the combination procedure are presented. The values of $F_2^{c\bar{c}}$ with statistical, uncorrelated and correlated uncertainties ordered by the particular source can be found in [11].

2.1 H1 Data

The measurements of $D^{*\pm}$ production cross sections and inclusive track measurements based on the vertex information using the HERA I and HERA II data are used in the combination.

The $D^{*\pm}$ cross-section measurement [6] corresponds to the data taking period of 1999-2000 with an integrated luminosity of $47\ pb^{-1}$ and covers the kinematic range of photon virtuality $2 < Q^2 < 100\ GeV^2$ and inelasticity $0.05 < y < 0.7$. The more recent cross section measurement [7] uses the full HERA II data of the 2004-2007 period corresponding to an integrated luminosity of 340 pb^{-1} and covers the kinematic range $5 < Q^2 < 1000\ GeV^2$, $0.02 < y < 0.7$. The details of the systematic studies in $D^{*\pm}$ analyses can be found elsewhere [6, 7]. Sources of totally correlated, uncorrelated and partially correlated experimental systematic uncertainties are distinguished.

- the following bin-to-bin correlated uncertainties are considered: electron energy E_e and polar angle θ_e, hadronic energy E_{had}, luminosity L, trigger efficiency, branching ratio for the decay channel $D^* \to KK\pi$, photoproduction background, stability of the efficiency due to the usage of RAPGAP or CASCADE Monte-Carlo Simulations.
- uncorrelated uncertainties: extraction of the $D^{*\pm}$ signal (fit shape), stability of the efficiencies due to the variation of the PDF in the Monte-Carlo, variation of the cut on the D^0 mass, contribution of reflections to the D^* signal, radiative corrections
- partially (50%) correlated uncertainties: tracking efficiency, reconstruction of the primary vertex.

The measurements of $F_2^{c\bar{c}}$ using the vertex detector (CST) information [8, 9] use the data from 1999-2000 and 2006-2007 running periods. The HERA I measurements correspond to the luminosity of $57.4\,pb^{-1}$ and cover the kinematic region of $12 < Q^2 < 60\,GeV^2$, $0.000197 < x < 0.005$. The HERA II data correspond to the luminosity of $189\,pb^{-1}$ and cover the kinematic range of $5 < Q^2 < 400\,GeV^2$ and $0.0002 < x < 0.013$. In these measurements the following uncertainty sources are considered:

- the following bin-to-bin correlated uncertainties are taken into account: impact parameter smearing, H1 drift chamber track finding efficiency, CST track finding efficiency, $D-$ and $B-$ multiplicities, c- and b-fragmentation, QCD model uncertainty, hadronic energy E_{had}, ϕ_{had}, normalization uncertainty, referring to the error of the luminosity measurement for the H1 F_2 measurement at HERA-I.
- the uncertainty arising from the light flavour background is treated as uncorrelated

Three systematic uncertainty sources are treated as cross-correlated between the $D^{*\pm}$ and the inclusive track measurements: H1 drift chamber track finding efficiency, hadron energy and the c-quark fragmentation.

2.2 ZEUS Data

The following ZEUS data have been included:

- $D^{*\pm}$ measurement from 1998-00 data [1].
  Luminosity $L = 82$ pb^{-1}. Visible cross sections for $1.5 < p_T^{D^*} < 15$ GeV and $|\eta^{D^*}| < 1.5$ in 31 bins of x and Q^2. $1.5 < Q^2 < 1000$ GeV^2. The $D^{*\pm}$ mesons were reconstructed in the "$K2\pi$" channel [1]. All the experimental uncertainties are treated as uncorrelated after an analysis of the correlations based on [2]. The $D^{*\pm}$ data have been corrected for the beauty contribution using the theoretical b cross sections reported in the corresponding papers.
- $D^{*\pm}$ measurement from 1996-97 data [3].
  $L = 37$ pb^{-1}. Visible cross sections for $1.5 < p_T^{D*} < 15$ GeV and $|\eta^{D*}| < 1.6$ in 21 bins of x and Q^2. $1 < Q^2 < 200$ GeV^2. Only the measurements in the "$K2\pi$" channel are considered in the combination. All the experimental uncertainties are treated as uncorrelated.
- $D^{0,\mathrm{no}D^{*+}}$ measurement from 2004-2005 period [5].
  $L = 134$ pb^{-1}. Here, $D^{0,\mathrm{no}D^{*+}}$ indicates D^0 mesons not originating from a $D^{*\pm}$ decay. Visible cross sections for $1.5 < p_T^D < 15$ GeV and $|\eta^D| < 1.6$ in 2×9 bins of x and Q^2. $5 < Q^2 < 1000$ GeV^2. The beauty contribution was already subtracted. The systematic uncertainty from the decay length significance and from the luminosity are taken as correlated between all the data points. Other experimental uncertainties, are treated as uncorrelated [17].

[1] A typo was found in Table 3 of the paper [1]: for the rows 22, 23 the y ranges should read 0.22-0.10 and 0.10-0.02, respectively

- Charm and beauty production in semi-leptonic decays into muons from 2005 data [4]. $L = 126\,pb^{-1}$. Visible muon cross sections for muons from charm decays, excluding charm from b decays, for $p_T^{\mu} > 1.5$ GeV, $-1.6 < \eta^{\mu} < 2.3$ in 8 bins of x and Q^2. $20 < Q^2 < 10000\,GeV^2$. The dominant sources of systematic uncertainty are taken as correlated: BRMUON efficiency, FMUON efficiency, energy scale, P_T^{miss} calibration, hadronic energy resolution, impact parameter resolution, MC model dependence. The other sources are considered as uncorrelated.

2.3 Extraction of $F_2^{c\bar{c}}$ from visible cross sections

The D meson and muon production cross sections measured in a given bin of x, Q^2 and in the visible phase space defined by the cuts on η and p_T of the D meson or of the muon ($\sigma_{\text{vis,bin}}^{\text{meas}}$) are transformed to $F_2^{c\bar{c}}$ at a reference x, Q^2 point ($F_2^{\text{c,meas}}(x, Q^2)$) as

$$F_2^{\text{c,meas}}(x, Q^2) = \sigma_{\text{vis,bin}}^{\text{meas}} \frac{F_2^{\text{c,model}}(x, Q^2)}{\sigma_{\text{vis,bin}}^{\text{model}}}. \tag{1}$$

using the NLO calculation at FFNS [12, 13].

For the H1 D^* measurements, the following model parameters (and variations) are used: charm mass $m_c = 1.43(1.3 - 1.6)\,GeV$, renormalisation and factorisation scales $\mu_r = \mu_f = \mu_0\sqrt{Q^2 + 4m_c^2}\,(0.5\mu_0 < \mu_r = \mu_f < 2\mu_0)$. The charm fragmentation function has been measured at H1 [15] using inclusive $D^{*\pm}$ meson production associated with jet production. Following the line of that measurement, the Kartvelishvili fragmentation function [16], which is controlled by a single parameter α, is used. The appropriate values of the fragmentation parameter are determined in Ref. [15] for the particular model. They depend on the center of mass energy of the hard process, $\hat{s}$. To obtain the visible $D^{*\pm}$ production cross sections in HVQDIS, charm quarks are fragmented in the photon - proton centre of mass frame into $D^{*\pm}$ mesons according to Kartvelishvili function using $\alpha = 6.0^{+1.1}_{-1.3}$ for $\hat{s} < 70$ GeV^2 and $\alpha = 3.3^{+0.4}_{-0.4}$ otherwise. The MRST2004FF3 [28] parton densities were used.

The model uncertainties on the $F_2^{c\bar{c}}$ values are determined by varying the charm mass, renormalisation and factorisation scales, parameters of the fragmentation function as described elsewhere [7]. Additional uncertainty of charm fragmentation fraction $fc \to D^{*\pm}$ of 2.9% is also taken into account. Arising model uncertainties are symmetrized and treated as bin-to-bin correlated. Additional uncertainty due to the extrapolation model used is accounted for. To estimate the latter, the extrapolation factors, determined as ratios of visible to the total $D^{*\pm}$ cross section are calculated using HVQDIS and CASCADE. In the highest x bins at $5 < Q^2 < 100$ GeV^2 these factors differ significantly. For the central value, the average $F_2^{c\bar{c}}$ obtained using HVQDIS and CASCADE models is taken. The highest x points are excluded. The half-difference of the CASCADE and HVQDIS extrapolated $F_2^{c\bar{c}}$ values are taken as a symmetric systematic uncertainty. This extrapolation uncertainty is treated as bin-to-bin correlated.

For the ZEUS measurements, the following parameters were used in HVQDIS for the extraction of $F_2^{c\bar{c}}$, with the variations reported in parenthesis.

1. PDF: ZEUS-S FFNS
2. scales: $\mu_f = \mu_r = \mu_0\,(0.5\mu_0, 2\mu_0)$ where $\mu_0 = \sqrt{Q^2 + 4m^2}$;

3. $\mu_c = 1.5\,(1.3, 1.7)$GeV;

4. Peterson fragmentation with:
$\epsilon(D^*) = 0.035\,(0.025, 0.085)$ and $\epsilon(\mu, D^+, D^{0,\mathrm{no}D^{*+}}) = 0.055\,(0.04, 0.12)$. The softer fragmentation for ground states and muons takes into account that they are partly originating from decays of D^*s or other excited states.

5. Fragmentation fractions:
$f(c-> D^{*+}) = 0.235 \pm 0.007$ [18],
$f(c-> D^{0,\mathrm{no}D^{*+}}) = 0.45^{+0.04}_{-0.03}$ [19],
$f(c-> D^+) = 0.216^{+0.029}_{-0.021}$ [19],
$f(c-> \mu^+) = 0.096 \pm 0.010$ [20].

6. Alternative fragmentation:
"jetset" fragmentation used instead of hvqdis [1], only for the $D^{*\pm}$ measurements.

The effect of the variation of the same parameter is considered as fully correlated among different H1 and ZEUS measurements. Although the parameters used to extract $F_2^{c\bar{c}}$ by H1 and ZEUS are not always the same, they have been considered to be sufficiently consistent to be treated as correlated for a preliminary result.

2.4 Combination Method

The combination of the data sets uses the χ^2 minimization method developed for the combination of inclusive DIS cross sections, as described in [21]. The χ^2 function takes into account the correlated systematic uncertainties for the H1 and ZEUS cross-section measurements. The χ^2 is defined as

$$\chi^2\left(\boldsymbol{m}, \boldsymbol{b}\right) = \sum_i \frac{\left(m^i - \sum_j \gamma^i_j m^i b_j - \mu^i\right)^2}{\left(\delta_{i,\mathrm{stat}}\,\mu^i\right)^2 + \left(\delta_{i,\mathrm{uncor}}\,m^i\right)^2} + \sum_j b_j^2\,. \tag{2}$$

Here μ^i is a measured value at a point i and γ^i_j, $\delta_{i,\mathrm{stat}}$ and $\delta_{i,\mathrm{uncor}}$ are relative correlated systematic, relative statistical and relative uncorrelated systematic uncertainties, respectively. The function χ^2 depends on the predictions m^i for the measurements (denoted as the vector $\boldsymbol{m}$) and on the shifts of correlated systematic error sources b_j (denoted as $\boldsymbol{b}$). Here $\mu^i = F^{c\bar{c}}_{2,i}(x_i, Q^2_i)$, where i denotes an particular measurement, and the summation over j extends over all correlated systematic sources. The predictions m^i are given by the assumption that the true value for a given (x, Q^2) point is the same for all the measurements referred to that particular point.

The combined data are obtained as the set of m^i corresponding to the minimum of χ^2 with respect to $\boldsymbol{m}$ and $\boldsymbol{b}$. Under the assumption that the statistical uncertainties are constant and that the systematic uncertainties are proportional to m^i, the minimum of Eq. 2 provides an unbiased estimator of $\boldsymbol{m}$.

In the present analysis the correlated and uncorrelated systematic uncertainties are of multiplicative nature, i.e. they increase proportionally to the central values. In Eq. 2 the multiplicative nature of these uncertainties is taken into account by multiplying the relative errors γ^i_j and $\delta_{i,\mathrm{uncor}}$ by the expectation m^i.

In the case inclusive DIS cross-section measurements, the background contribution is small and the statistical uncertainties are proportional to the square root of the number of signal events. In contrary, in the charm analyses the statistical uncertainty is mainly background dominated and therefore it is treated as constant, i.e. independent on m_i .

The original double differential cross-section measurements are published with their statistical and systematic uncertainties. The statistical uncertainties correspond to $\delta_{i,\mathrm{stat}}$ in Eq. 2. The systematic uncertainties are classified as either point-to-point correlated or point-to-point uncorrelated, corresponding to γ_i^j and $\delta_{i,\mathrm{uncor}}$, respectively. Asymmetric systematic uncertainties are symmetrised before performing the averaging. The resulting average is found to be insensitive to the details of the symmetrisation procedure.

Experimental systematic uncertainties are treated as independent between H1 and ZEUS. Model uncertainties due to variation of charm quark mass and renormalisation and factorisation scales, charm fragmentation as well as branching fractions are treated as correlated. All the $F_2^{c\bar{c}}$ data from H1 and ZEUS are combined in one simultaneous minimisation.

2.5 Extrapolation to Common $x - Q^2$ Grid

Prior to the combination, the H1 and ZEUS data are transformed to a common grid of (x, Q^2) points. The grid points are chosen such that the interpolation corrections are minimal taking advantage of the fact that the original (x, Q^2) grids of the H1 and ZEUS experiments are similar. Furthermore, the chosen grid ensures that no two separate measurements of the same data set interpolate to a common grid point

For the majority of the grid points both H1 and ZEUS measurements enter. For some of the grid points there is no nearby counterpart from the other experiment, giving points in the combined cross section which originate from either H1 or ZEUS only. Note that through the systematic error correlation, such data points may be nevertheless shifted with respect to the original measurement in the averaging procedure.

The transformation of a measurement from the given (x, Q^2) to the nearest $(x_{\mathrm{grid}}, Q^2_{\mathrm{grid}})$ point on the grid is performed by multiplying the measured cross section by a ratio of theoretically calculated $F_2^{c\bar{c}}$ values at $(x_{\mathrm{grid}}, Q^2_{\mathrm{grid}})$ and (x, Q^2). This interpolation is performed using the NLO FFNS QCD calculation [12] using MRST2004FF3 parton density set, charm mass of $1.43\ GeV$ and renormalisation and factorisation scales $\mu_r = \mu_f = \sqrt{Q^2 + 4m_c^2}$.

2.6 Procedural Uncertainties

The χ^2 function given by Eq. 2 treats all systematic uncertainties as multiplicative, i.e. proportional to the expected central values. While this generally holds for the normalisation uncertainties, this may not be the case for the other uncertainties. To study the sensitivity of the average result to this issue, an alternative averaging is performed, for which only correlated uncertainties are taken as multiplicative while the uncorrelated uncertainties are treated as additive. In addition, the averaging is performed where the statistic uncertainty is treated as proportional to the square root of the central value.

The difference between the values of these averaging results and the nominal average result is taken into account as an asymmetric procedural error $\delta_{\mathrm{ave,rel}}$ and is added to the total uncertainty of the averaging result in quadrature.

2.7 Alternative Combination Method

An alternative combination program [22] based on the Bayesian Analysis Toolkit [23] was also used. The main application of the program is to combine data or to fit datasets with correlated systematics using a Bayesian approach. In the Bayesian approach the probability density for the true values $\mathbf{m}$ is given by

$$f(\mathbf{m}) \propto \int d\mathbf{b}\, p(\mu|\mathbf{m},\mathbf{b})\, f_0(\mathbf{m})\, f_0(\mathbf{b})$$

where the likelihood $p(\mu|\mathbf{m},\mathbf{b})$ is the probability for obtaining the measured values μ given the true values and the systematic shifts $\mathbf{b}$. $f_0(\mathbf{m})$ and $f_0(\mathbf{b})$ indicates the a-priori distributions.

Before performing a full Bayesian combination, the program was used to make a check of the standard procedure. To do this, a simplified likelihood (all uncertainties not dependent on m) defined as

$$p(\mu|\mathbf{m},\mathbf{b}) = \prod_i \exp\left(-\frac{(\mu^i - \sum_j \mu^i \gamma^i_j b_j - m^i)^2}{2(\mu^i)^2(\delta^2_{\text{stat}} + \delta^2_{\text{uncor.}})}\right)$$

was used, with $f_0(\mathbf{m})$ =const and $f_0(\mathbf{b}) = \prod_j \exp(-b_j^2/2)$. The global mode of $f(\mathbf{m})$, obtained using Minuit, was then compared with the results of the standard combination repeated using constant uncertainties.

3 Results

The full list of the 54 systematic sources, and the averaged $F_2^{c\bar{c}}(x,Q^2)$ with correlated, uncorrelated, total and procedural uncertainties can be found in [11]. The shifts of correlated systematic uncertainties ordered by the error source are also given in [11]. In general, the shifts are much smaller than the uncertainty value and in 4 cases exceed this value by less about 10%. The total χ^2/n_{dof} of the averagig procedure amonuts to $88/110$. The cross-correlated uncertainties between H1 and ZEUS are significantly reduced. The combined values of $F_2^c(x,Q^2)$ are shown in Figs. 1 and 2, on top of existing results of H1 and ZEUS collaborations used in the averaging procedure. The combined values of $F_2^{c\bar{c}}$ are compared to NLO FFNS predictions in Fig. 3 and 4, to GMVFNS predictions of the global PDF fits in Fig. 5 and 6. The comparison of the data with the combilation recent theory calculations is shown in Fig. 7.

References

[1] S. Chekanov *et al.* [ZEUS Collaboration], Phys. Rev. D **69** (2004) 012004 [arXiv:hep-ex/0308068].

[2] S. Chekanov, S. Robins, M. Wing "Measurement of D* Cross Sections and the Charm Structure Function of the Proton in DIS at HERA", ZEUS Note 05-016.

[3] J. Breitweg *et al.* [ZEUS Collaboration], Eur. Phys. J. C **12** (2000) 35 [arXiv:hep-ex/9908012].

[4] S. Chekanov *et al.* [ZEUS Collaboration], arXiv:0904.3487 [hep-ex], accepted by Eur. Phys. J. C.

[5] S. Chekanov *et al.* [ZEUS Collaboration], Eur. Phys. J. C **63** (2009) 171 [arXiv:0812.3775 [hep-ex]].

[6] A. Aktas *et al.* [H1 Collaboration], Eur. Phys. J. **C51** (2007) 271.

[7] [H1 Collaboration] H1 Preliminary 08-074
[H1 Collaboration] H1Preliminary 08-072
[H1 Collaboration] H1 Preliminary H1-08-172
[H1 Collaboration] H1 Preliminary H1-08-173

[8] A. Aktas *et al.*[H1 Collaboration] Eur. Phys. J. **C**45 (2006) 23

[9] [H1 Collaboration] H1 Preliminary H1-08-173

[10] C. Adloff *et al.* (H1 Collaboration), Nucl. Phys. B545 (1999) 21.

[11] https://www.desy.de/h1zeus/heavy-flavour/results.html

[12] E. Laenen *et al.*, Phys. Lett. B291 (1992) 325.
E. Laenen *et al.*, Nucl. Phys. B392 (1993) 162, 229;
S. Riemersma, J. Smith, and W.L. van Neerven: Phys. Lett. B347 (1995) 143.

[13] B.W. Harris and J. Smith, Phys. Rev. D57 (1998) 2806.

[14] H. Jung and G. P. Salam, Eur. Phys. J. **C19** (2001) 351 [arXiv:hep-ph/0012143];
H. Jung, Comp. Phys. Commun.**143 100** (2002) 143 [arXiv:hep-ph/0109102].

[15] A. Aaron *et al.* [H1 Collaboration], Eur. Phys. J. **C59** (2009) 589.

[16] V. G. Kartvelishvili, A. K. Likhoded and V. A. Petrov, *Phys. Lett.* B**78** (1978) 615.

[17] D. Nicholass, Ph.D Thesis (UCL) 2008, DESY-THESIS-08-046.

[18] L. Gladilin, arXiv:hep-ex/9912064.

[19] S. Chekanov *et al.* [ZEUS Collaboration], JHEP **0707** (2007) 074 [arXiv:0704.3562 [hep-ex]].

[20] C. Amsler *et al.* [Particle Data Group], Phys. Lett. B **667**, 1 (2008).

[21] F. Aaron *et al.*[H1 Collaboration] (2009), [arXiv:0904.0929]

[22] "Combine", the code is available from
`http://www-zeus.desy.de/ corradi/Combine`
or by contacting `massimo.corradi@bo.infn.it`

[23] A. Caldwell, D. Kollar, K. Kröninger, Comp. Phys. Comm. **180** (2009) 2197-2209, see also `http://www.mppmu.mpg.de/bat`

[24] S. Alekhin, J. Blümlein, S. Klein, S. Moch [arXiv:0908.3128]
S. Alekhin, J. Blümlein, S. Klein, S. Moch [arXiv:0811.1412]
S. Alekhin, J. Blümlein, S. Klein, S. Moch [arXiv:0811.1412]

[25] M.Glück, P. Jimenez-Delgado,E. Reya, C.Schuck [arXiv:0801.3618]

[26] G. Watt, A. D. Martin, W. J. Stirling, R. S. Thorne [arXiv:0806.4890]

[27] P. M. Nadolsky *et al.*, *Phys. Rev.* D78 (2008) 013994

[28] A. D. Martin, W. J. Stirling, and R. S. Thorne, *Phys. Lett.* B**636** (2006) 259.

[29] H. L. Lai *et al.*, Eur. Phys. J. **C12** (2000) 375 [arXiv:hep-ph/9903282].

[30] R. S. Thorne, C. D. White [arXiv:hep-ph/0611204v1].

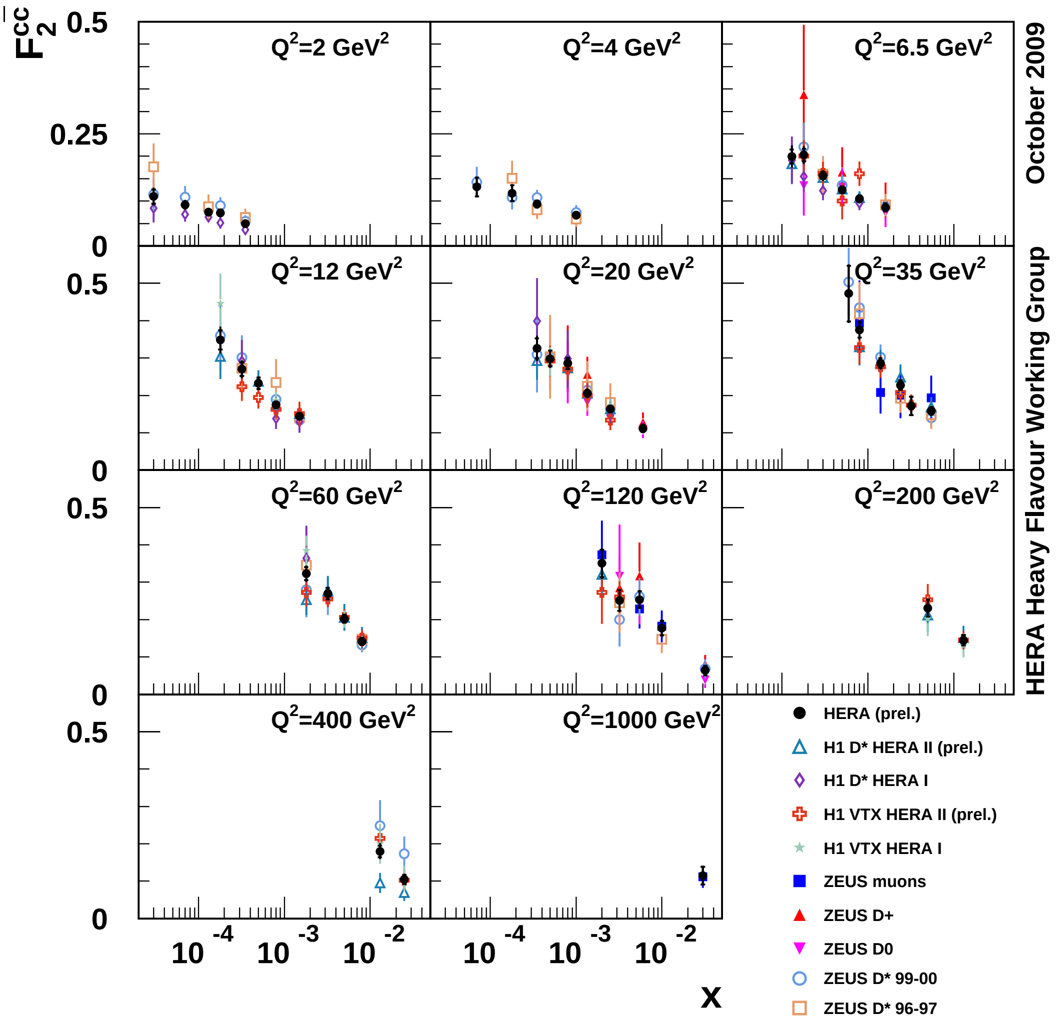

Figure 1: Charm contribution to the proton structure function, $F_2^{c\bar{c}}$, as a function of x in bins of Q^2. The averaged HERA $F_2^{c\bar{c}}$ (black circles) is compared to the data sets of the H1 and ZEUS measurement used for the combination. The different measurements are interpolated to the the common Q^2, x-values. The inner (full) error bars of the averaged value represent the uncorrelated (total) uncertainties.

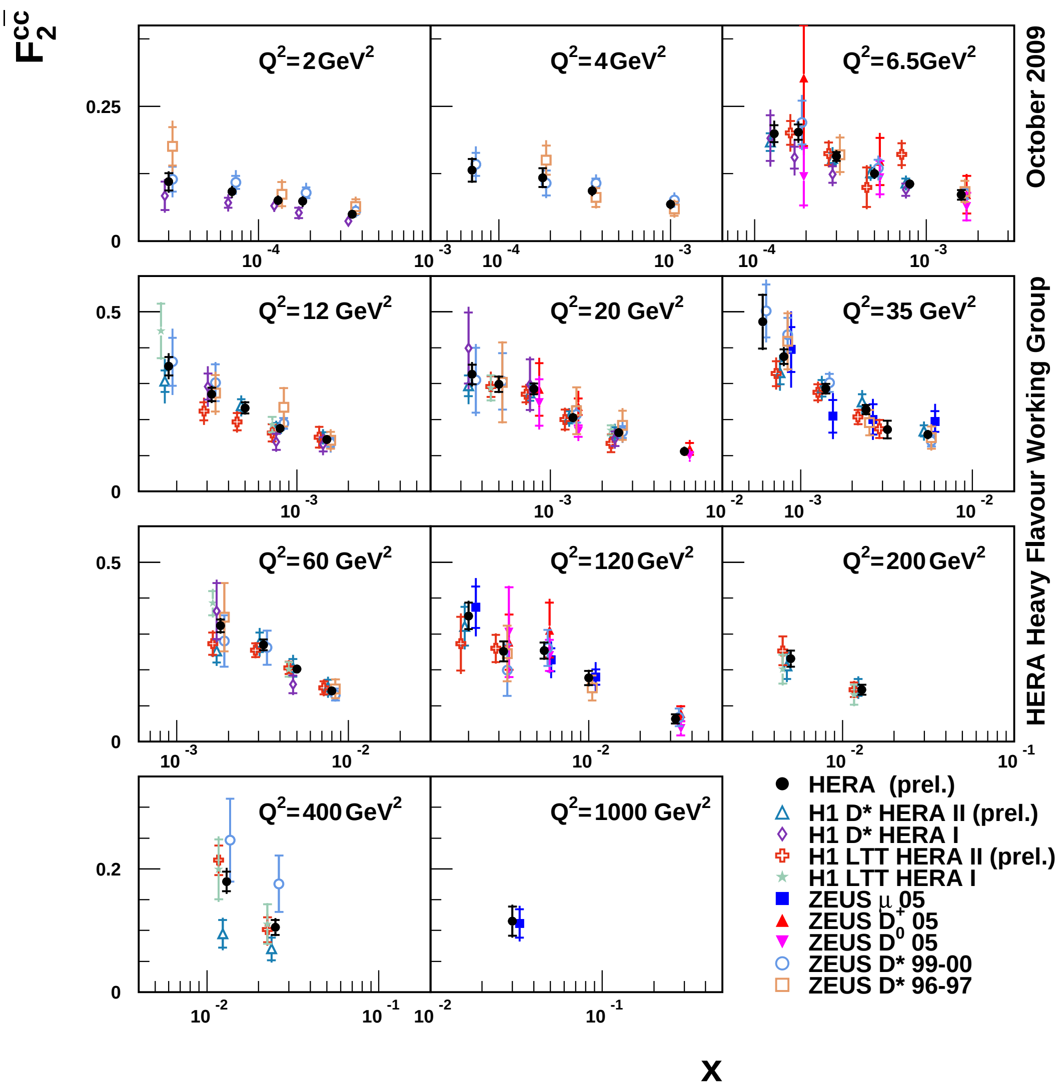

Figure 2: Charm contribution to the proton structure function, $F_2^{c\bar{c}}$, as a function of x in bins of Q^2. The averaged HERA $F_2^{c\bar{c}}$ (black circles) is compared to the data sets of the H1 and ZEUS measurement used for the combination. The different measurements are interpolated to the the common Q^2, x-values. The inner (full) error bars of the averaged value represent the uncorrelated (total) uncertainties.

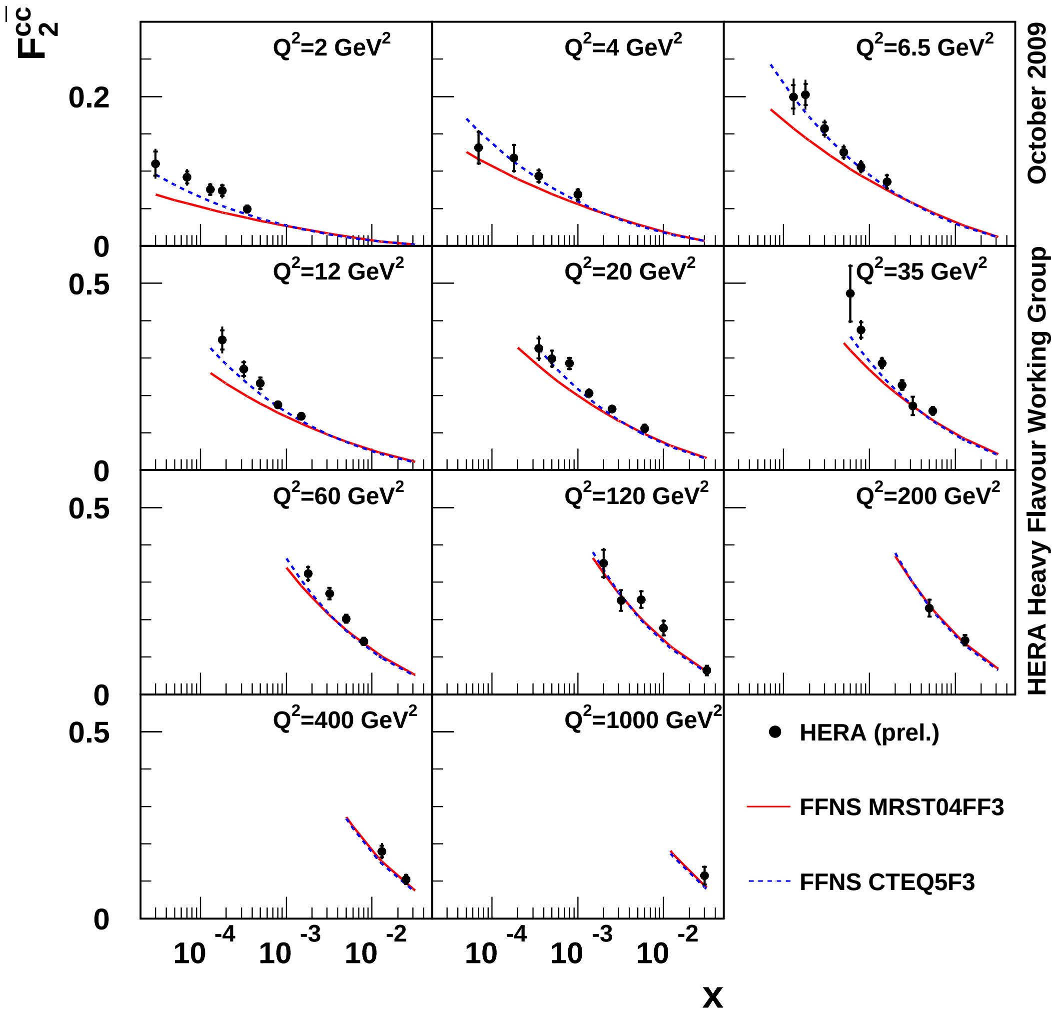

Figure 3: HERA Averaged $F_2^{c\bar{c}}$ as a function of x in Q^2 bins compared to the QCD prediction [12] at NLO in FFNS as used for the swimming to the common grid. The data (closed symbols) are shown with the uncorrelated (inner error bars) and the total (full error bars) uncertainties. Calculations using the the parton density sets MRST2004FF3 [28] (solid) and CTEQ5F3 [29] (dashed) are shown.

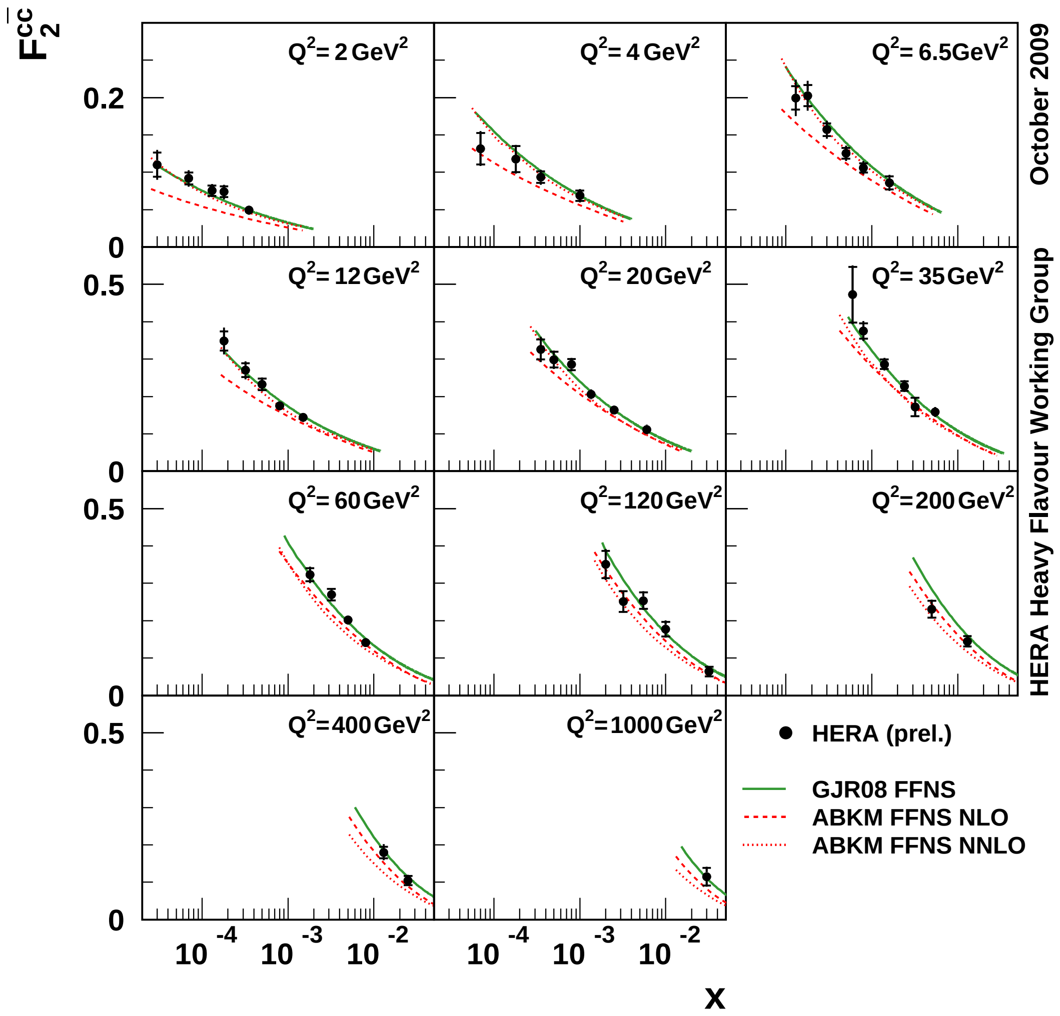

Figure 4: HERA Averaged $F_2^{c\bar{c}}$ (solid symbols) as a function of x in Q^2 bins compared to QCD predictions in FFNS. The data (closed symhown with the uncorrelated (inner error bars) and the total (full error bars) uncertainties. The predictions of ABKM [24] at NLO (dashed) and NNLO (dotted) and GJR08 [25] (light solid) are shown.

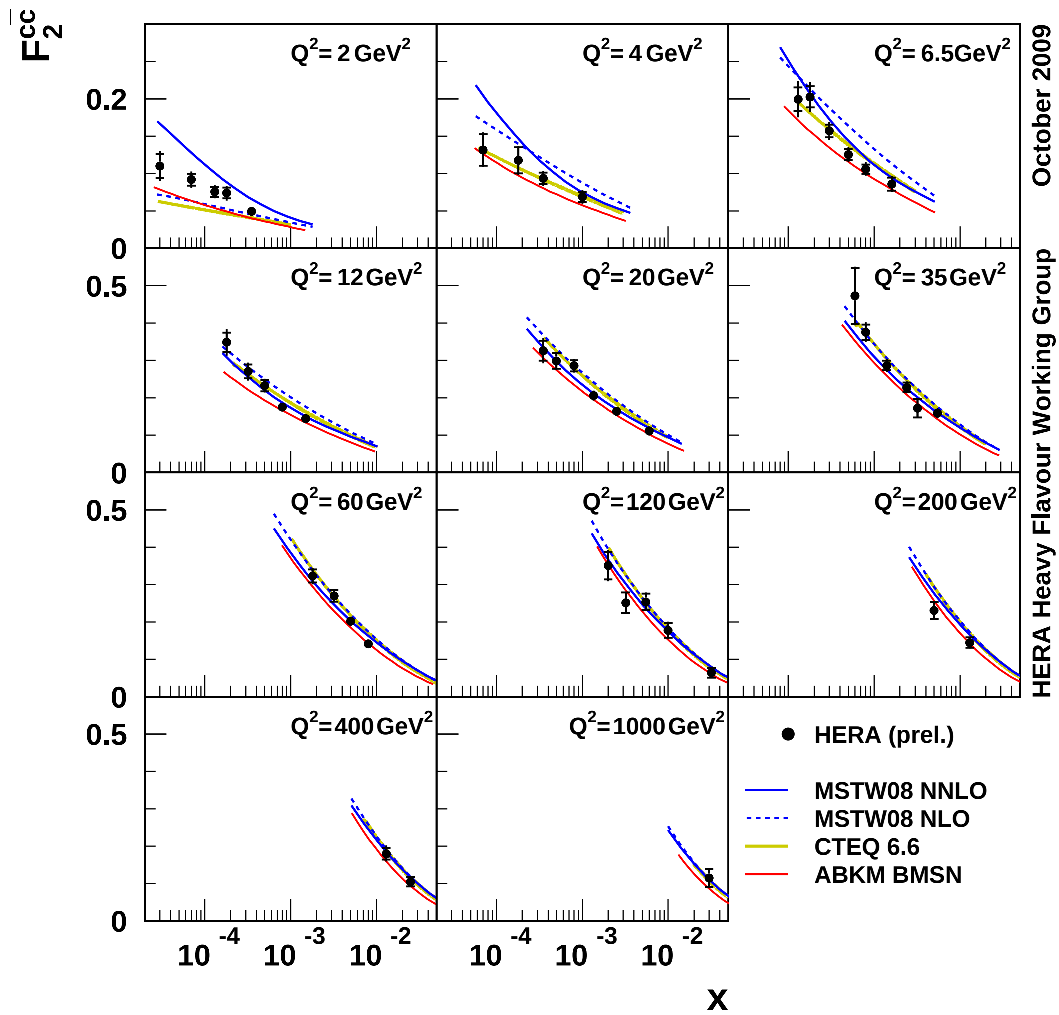

Figure 5: HERA Averaged $F_2^{c\bar{c}}$ as a function of x in Q^2 bins compared to QCD predictions in GMVFNS. The data (closed symbols) are shown with the uncorrelated (inner error bars) and the total (full error bars) uncertainties. Predictions from the global fit analyses of ABKM [24] (red), MSTW08 [26] at NLO(blue dashed) and NNLO (blue solid) and CTEQ 6.6 [27] (magenta) are shown.

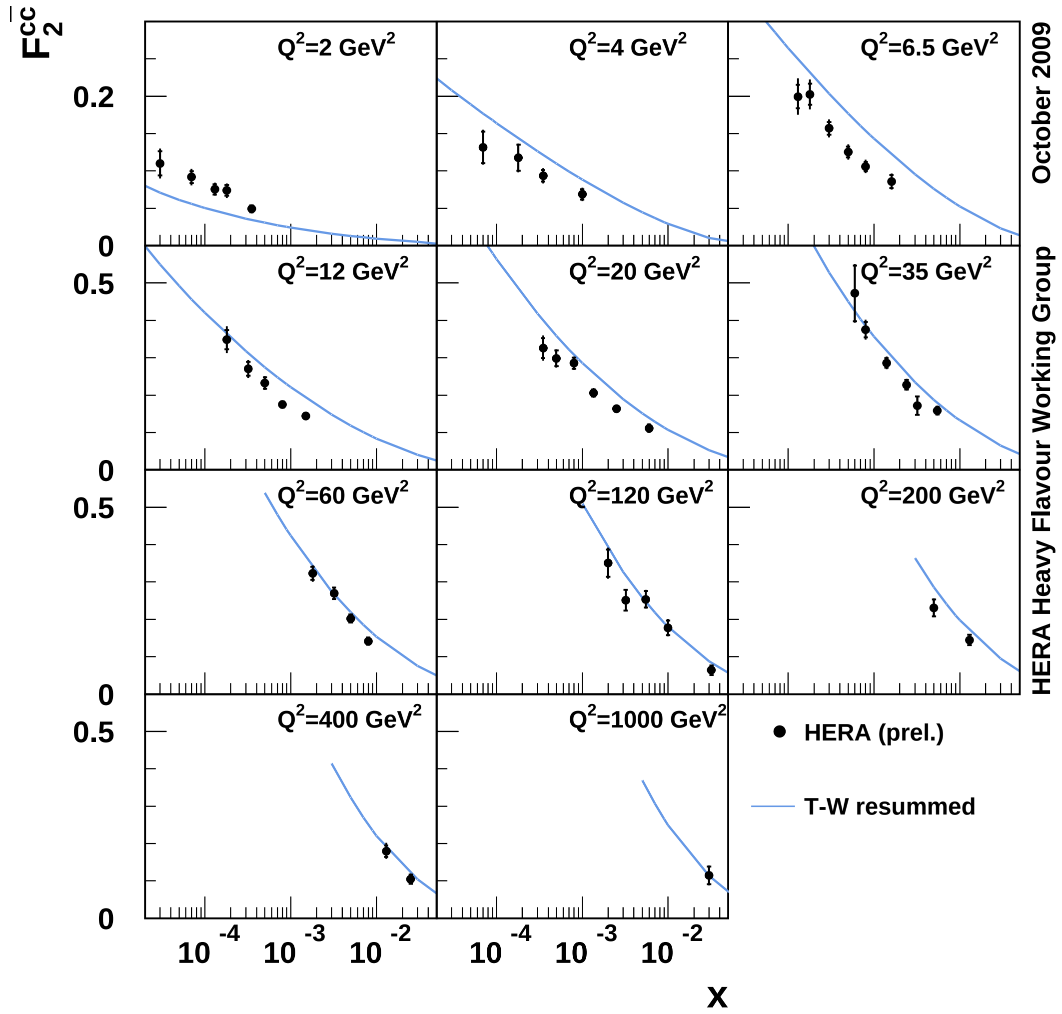

Figure 6: HERA Averaged $F_2^{c\bar{c}}$ as a function of x in Q^2 bins compared to QCD predictions in GMVFNS. The data (closed symbols) are shown with the uncorrelated (inner error bars) and the total (full error bars) uncertainties. The resummed calculation [30] is shown.

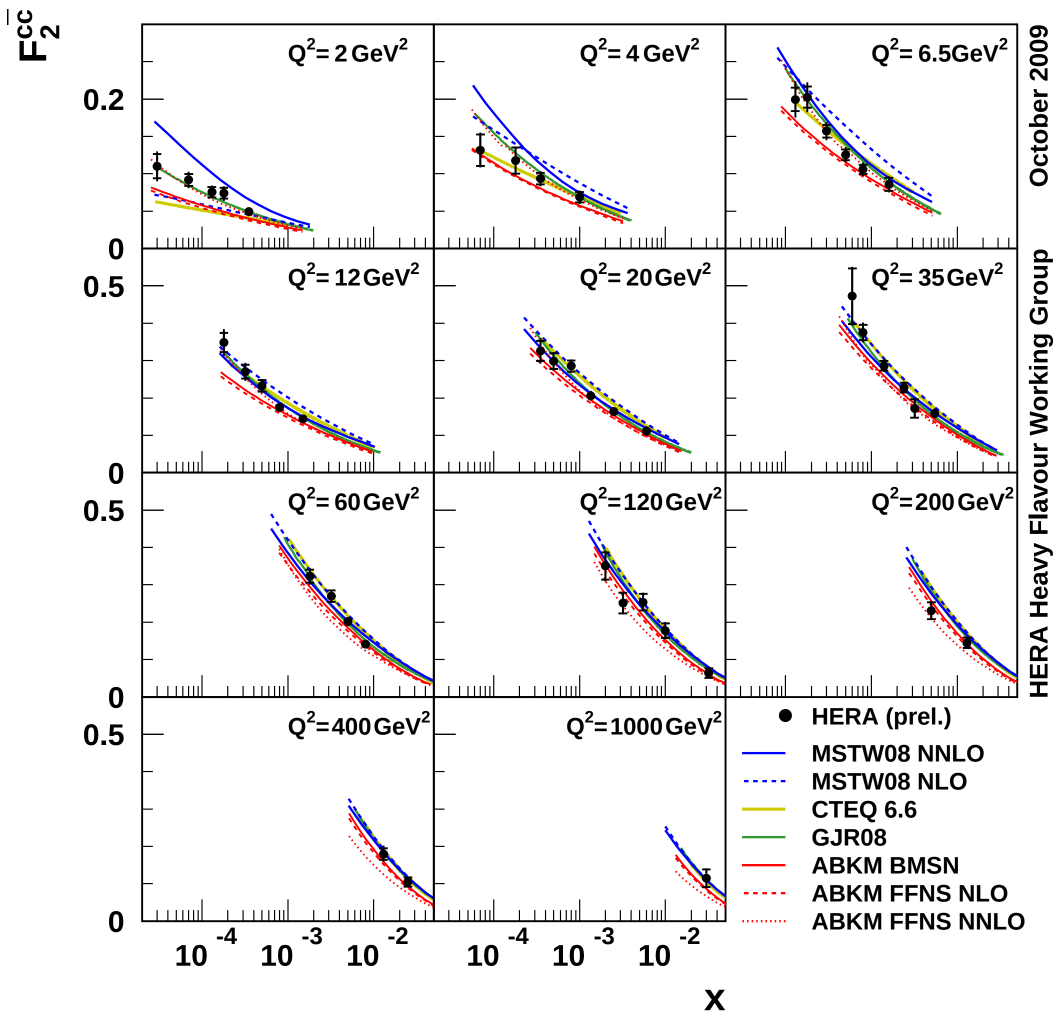

Figure 7: HERA Averaged $F_2^{c\bar{c}}$ as a function of x in Q^2 bins compared to recent QCD predictions in GMVFNS and FFNS. The data (closed symbols) are shown with the uncorrelated (inner error bars) and the total (full error bars) uncertainties. Predictions from the global fit analyses of ABKM [24], MSTW08 [26] at NLO and NNLO and CTEQ 6.6 [27] as well as GJR08 [25] are shown.